Lecture 4

Pore Pressure at Depth in sedimentary basins

(6 April, 8 April 2020)

Ki-Bok Min, PhD

Professor
Department of Energy Resources Engineering
Seoul National University

SEOUL NATIONAL UNIVERSITY

Introduction
Outline

- Pore Pressure at depth in sedimentary basins;
  - Importance and definition of pore pressure
  - Reservoir compartmentalization
  - Mechanisms of overpressure generation
  - Estimating pore pressure at depth

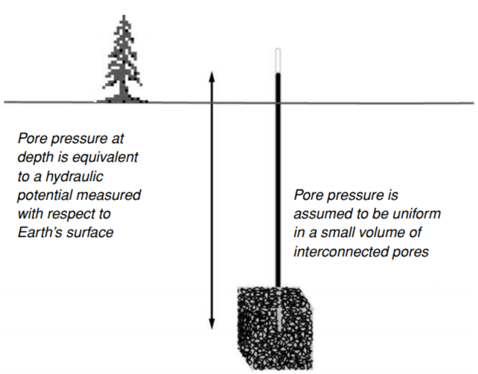

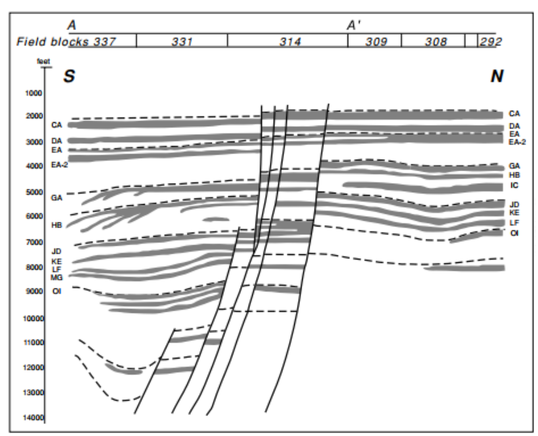

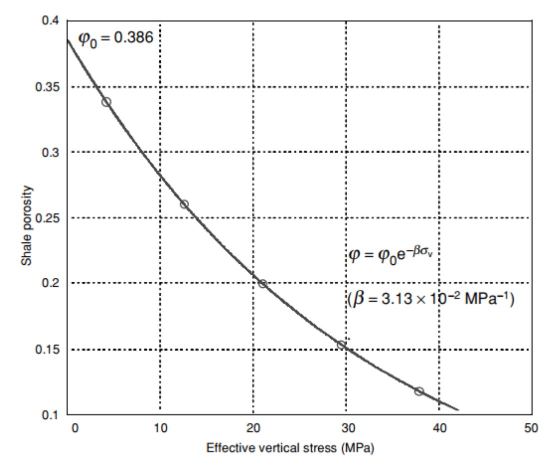

Zoback MD, 2007, Reservoir Geomechanics, Cambridge University Press

Definition and importance

SEOUL NATIONAL UNIVERSITY

- Pore pressure & stress magnitudes are closely coupled
  - Effective stress
  - Pore pressure vs. stress
- Drilling
  - Constraints on drilling Mud density (Mud weight window)
- Maximum hydrocarbon column height
- Reduction in reservoir pore pressure with production (depletion)
  - Deformation, compaction, and permeability loss
  - Induce faulting (seismicity)

Definition and importance

- Pore pressure
  - Scalar hydraulic potential acting within an interconnected pore psace at depth
  - Hydrostatic pressure: 10 MPa/km or 0.44 psi/ft

$$P_p^{\mathrm{hydro}} \equiv \int_0^z \rho_w(z) g \mathrm{d}z \approx \rho_w g z_w \qquad (2.1)$$

- Magnitude of pore pressure
  - Overpressure
  - Upper bound: overburden stress, S_v
  - The ratio of pore pressure to the vertical stress $\lambda_p = P_p/S_v$
  - Lithostatic pore pressure: $P_p = S_v$
  - The following will hold always: $P_p < S_3$
    - Because tensile rock strength is usually small
  - Assumption: pore pressure in quasi-static

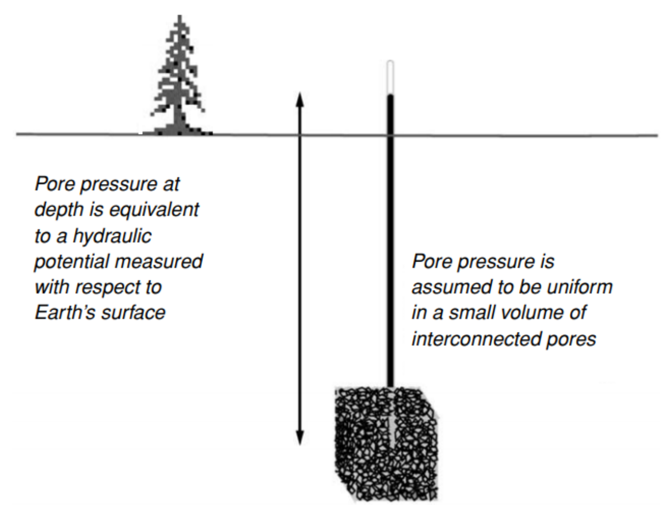

Figure 2.1. Pore pressure at depth can be considered in terms of a hydraulic potential defined with reference to earth's surface. Conceptually, the upper bound for pore pressure is the overburden stress, S_v.

Zoback MD, 2007, Reservoir Geomechanics, Cambridge University Press

Definition and importance

SEOUL NATIONAL UNIVERSITY

- Monte Cristo field (Gulf of Mexico)
  - Typical example of pore pressure variation (and overpressure)
  - Zone with >8000 ft is isolated from the shallow zone
  - Hard pore pressure: $P_p \sim S_v$
  - $\lambda_p = P_p/S_v$?

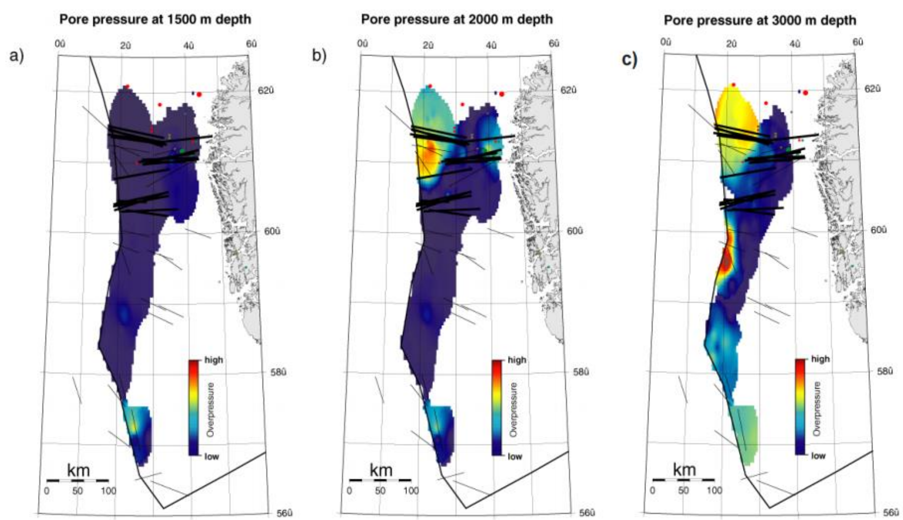

Pore pressure can change at a given depth from one area to another (Norwegian sector of northern North Sea)

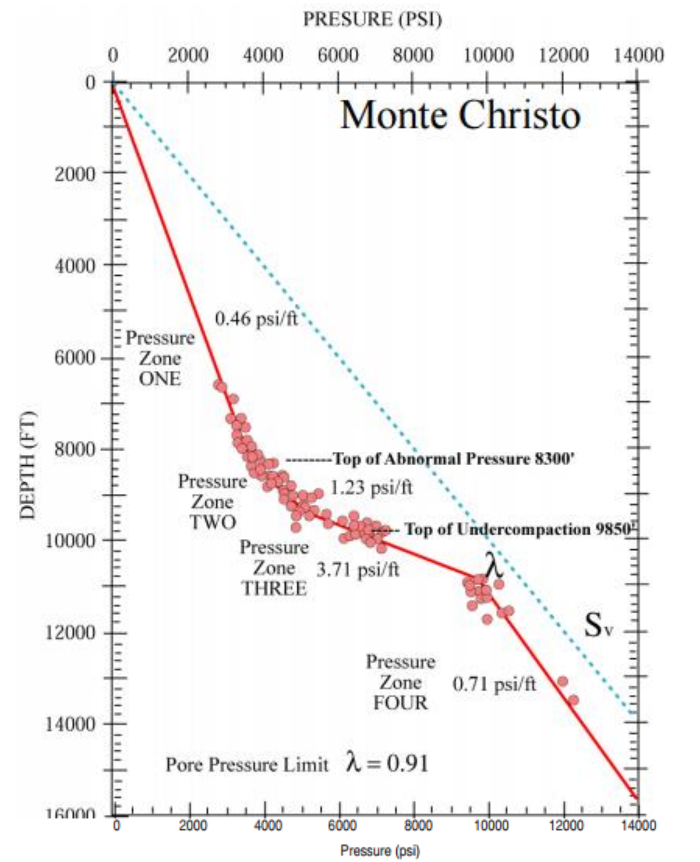

Figure 2.2. Pore pressure measurements in the Monte Cristo field, located onshore near the Gulf of Mexico in south Texas (after Engelder and Leftwich 1997). Such data are typical of many sedimentary basins in which overpressure is encountered at depth. Hydrostatic pore pressures is observed to a certain depth (in this case ~8300 ft), a transition zone is then encountered in which pore pressure increases rapidly with depth (in this case at an apparent gradient of 3.7 psi/ft) and extremely high pore pressures are observed at depths greater than ~11,000 ft. *AAPG© 1997 reprinted by permission of the AAPG whose permission is required for futher use.*

Zoback MD, 2007, Reservoir Geomechanics, Cambridge University Press

Reservoir Compartmentalization
Case in Northern Egypt

SEOUL NATIONAL UNIVERSITY

- A reservoir can be compartmentalized
  - A series of permeable sands + impermeable shales
  - Hydrostatic or overpressure
  - Pressure increase is hydrostatic wi each compartment
  - Mud weight: between P_p & S_3

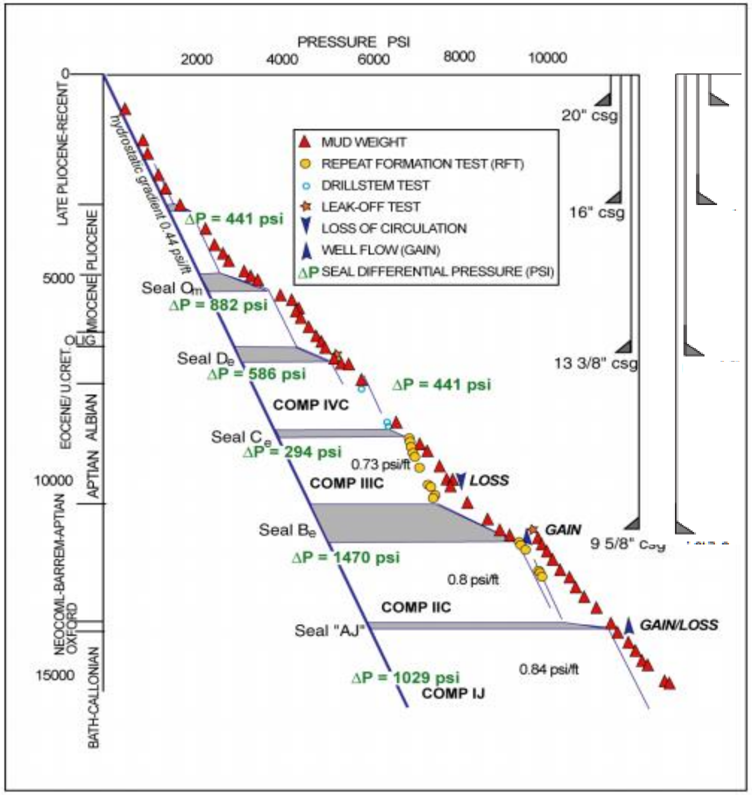

Figure 2.4. Pore pressure, mud weight and related parameters in the Mango-1 well in northern Egypt (after Nashaat 1998). The pore pressure measurements in compartments IIC and IIIC confirm that pore pressure increases with a local hydrostatic gradient within a compartment even though the absolute value of pore pressure is well above normal pressure values. *AAPG© 1998 reprinted by permission of the AAPG whose permission is required for futher use.*

Drillstem test: 산출시험

Zoback MD, 2007, Reservoir Geomechanics, Cambridge University Press

Reservoir Compartmentalization
Case in Gulf of Mexico (oil/gas/water)

SEOUL NATIONAL UNIVERSITY

- South Eugene Island (SEI) Block 330, Gulf of Mexico
  - Young (Pliocene-Pleistocene < 4 million years)
  - Sand & Shale
  - Data at SEI330 act as separate reservoir

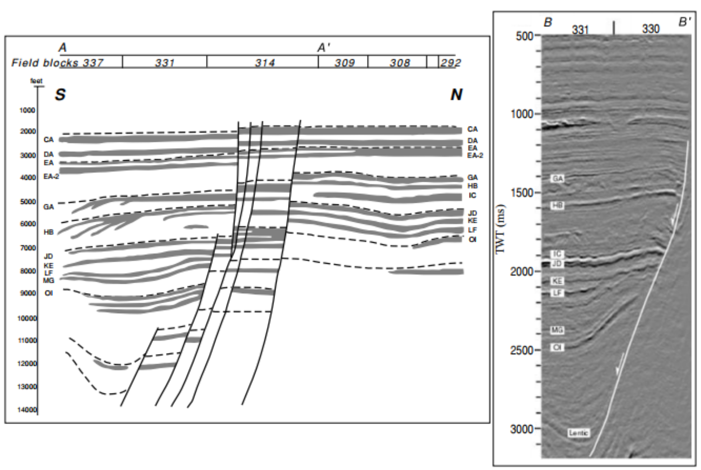

Figure 2.6. Geologic cross-section along line A–A′ in Figure 2.5 and a seismic cross-section along section B–B′ (modified after Alexander and Flemings 1995 and Finkbeiner, Zoback *et al.* 2001). In the geologic cross-section the permeable sands are shown in gray, shales are shown in white. Individual sands are identified by the alphabetic nomenclature shown. Note that slip decreases markedly along the *growth* faults as they extend upward. *AAPG© 1995 and 2001 reprinted by permission of the AAPG whose permission is required for futher use.*

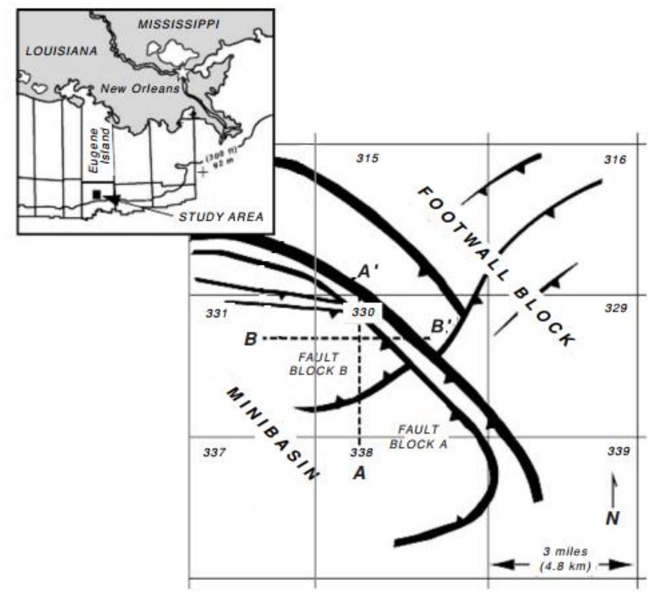

Figure 2.5. Map of the South Eugene Island (SEI) 330 field in the Gulf of Mexico (modified after Finkbeiner, Zoback *et al.* 2001). SEI 330 is one of the world's largest Plio-Pleistocene oil and gas fields. Studies of pore pressure, *in situ* stress and hydrocarbon migration in SEI 330 are referred to in subsequent chapters. *AAPG© 2001 reprinted by permission of the AAPG whose permission is required for futher use.*

Zoback MD, 2007, Reservoir Geomechanics, Cambridge University Press

Supplementary #1
Geologic Time

SEOUL NATIONAL UNIVERSITY

- Reservoir Engineers must be familiar with Geology

– 캄오실데 석탄 페노으면 트김쥐포백마리 제3기 제4기

come

Precambrian | Paleozoic (고생대) | Mesozoic (중생대) | Cenozoic (신생대)

Table 2.1 DIVISIONS OF GEOLOGIC TIME

Era (代)	Period (紀)	Epoch (世)	Absolute Age (million yr)
Cenozoic 신생대	Quaternary 제4기	Recent (Holocene) 홀로세	
		Pleistocene 플라이스토세	
			3
	Tertiary 제3기	Pliocene 플라이오세	
		Miocene 마이오세	
		Oligocene 올리고세	
		Eocene 에오세	
		Paleocene 팔레오세	
			70
Mesozoic 중생대	Cretaceous 백악기		
	Jurassic 쥬라기		
	Triassic 트라이아스기		
			230
Paleozoic 고생대	Permian 페름기		
	Carboniferous 석탄기	Pennsylvanian	
		Mississippian	
			350
	Devonian 데본기		
	Silurian 사일루리아기		
	Ordovician 오르도비스기		
	Cambrian 캄브리아기		
			600
Precambrian			Earlier

Source: Data from Verhoogen et al. (1970).

지질시대명의 시층서명의
(代)Era – Erathem (代/層)
Period (紀) – System (系)
Epoch (世) – Series (統)

Goodman RE, 1993, Engineering Geology, Wiley

Reservoir Compartmentalization
Case in Gulf of Mexico (oil/gas/wate

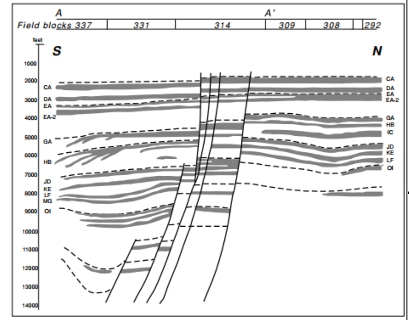

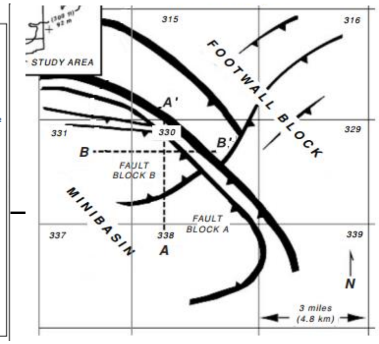

- Structure Contour Map (OI sand)
  - one of deeper producing intervals
  - Divided into different fault blocks
  - Distribution of water, oil (green) and gas (red) are markedly different in adjacent fault blocks
  - Oil columns at Fault block B, C vs. A, D, E are different

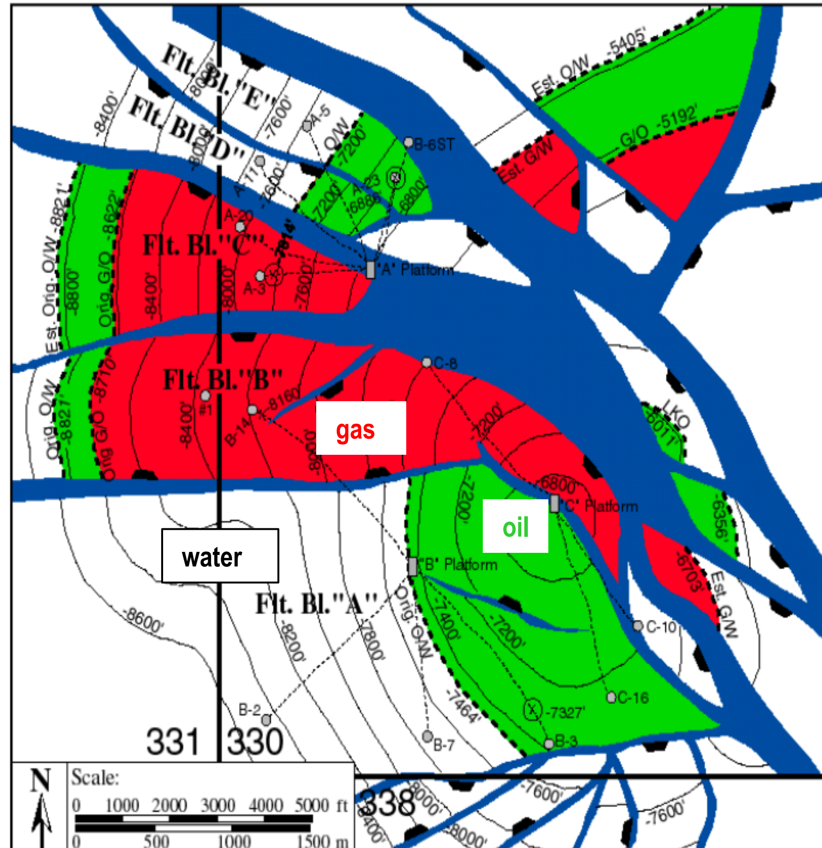

Figure 2.7. Structure contour map of the OI sand in the SEI 330 field (modified after Finkbeiner, Zoback *et al.* 2001). On the down-thrown side (hanging wall) of the major fault striking NW–SE, the sand is divided into structural fault blocs (A, B, C, D and E) based on seismically identified faults. Note the markedly different oil and gas columns in some of the fault blocks shows clear evidence of the compartmentalization of the OI reservoir. Oil is indicated shading, gas by stippling. *AAPG© 2001 reprinted by permission of the AAPG whose permission is required for futher use.*

Zoback MD, 2007, Reservoir Geomechanics, Cambridge University Press

Reservoir Compartmentalization
Case in Gulf of Mexico (oil/gas/wate

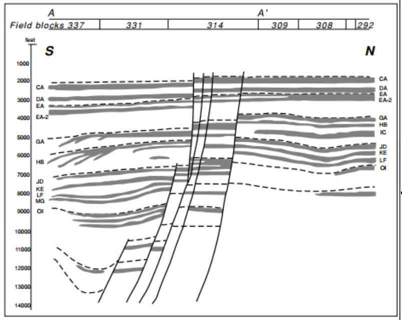

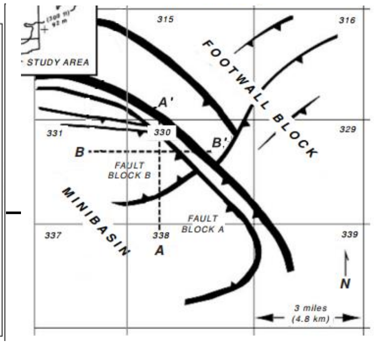

- Structure Contour Map (OI sand)

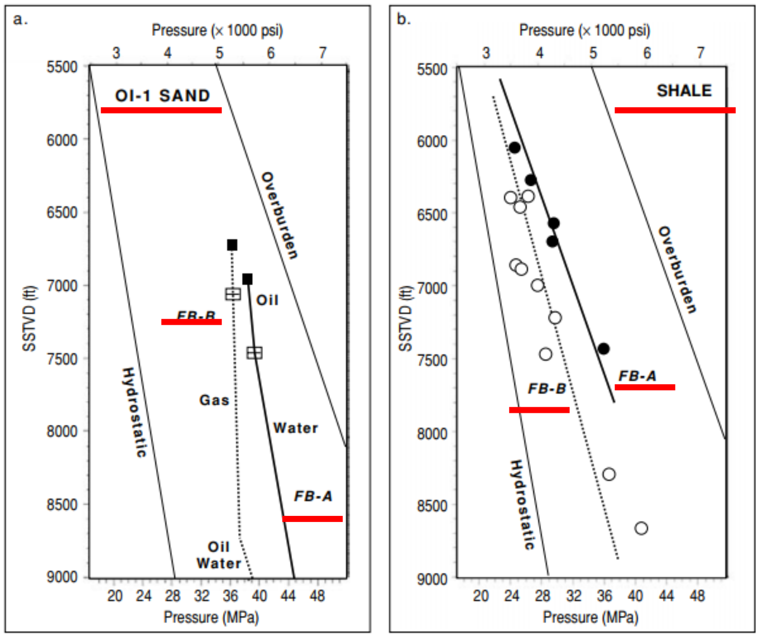

Figure 2.8. (a) Variations of pressure with depth in the OI sand based on direct measurements and extrapolations based on known column heights and fluid densities (Finkbeiner, Zoback *et al*. 2001). Note the markedly different pressures and hydrocarbon columns in these two adjacent fault blocks. Fault block A has a markedly higher water phase pressure and smaller hydrocarbon columns. (b) Shale pore pressures estimated from geophysical logs and laboratory studies of core compaction (after Flemings, Stump *et al*. 2002). Note that shale pressure is also higher in the fault block (FB)-A.

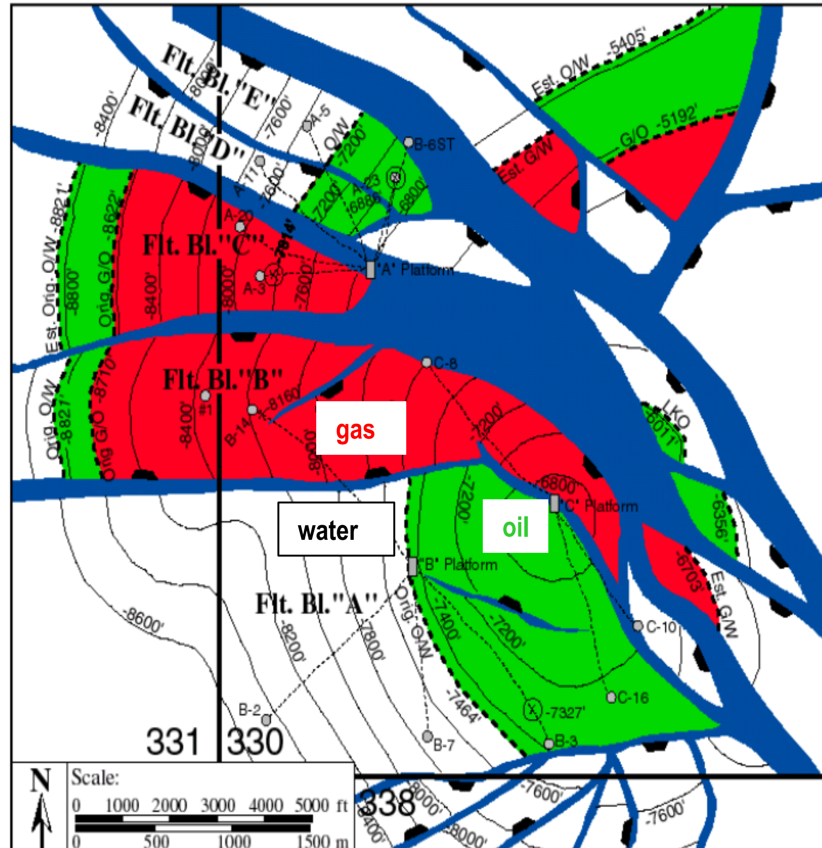

Figure 2.7. Structure contour map of the OI sand in the SEI 330 field (modified after Finkbeiner, Zoback *et al*. 2001). On the down-thrown side (hanging wall) of the major fault striking NW–SE, the sand is divided into structural fault blocs (A, B, C, D and E) based on seismically identified faults. Note the markedly different oil and gas columns in some of the fault blocks shows clear evidence of the compartmentalization of the OI reservoir. Oil is indicated shading, gas by stippling. *AAPG© 2001 reprinted by permission of the AAPG whose permission is required for futher use.*

Zoback MD, 2007, Reservoir Geomechanics, Cambridge University Press

Reservoir Compartmentalization
Pore pressure **variation** within compartments (1)

- P_p variation with depletion (SEI330)
  - SAND1 & SAND2 are not far away but their responses are different

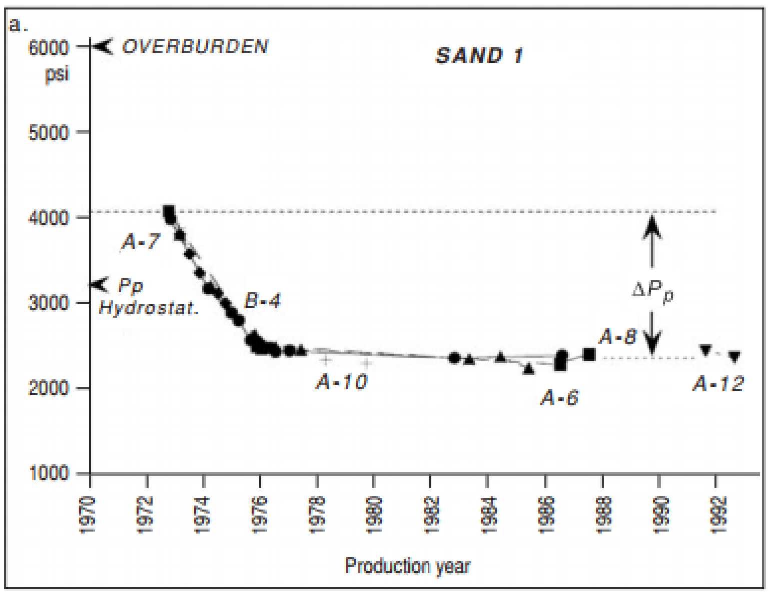

- P_p responds like a single interconnected hydraulic unit

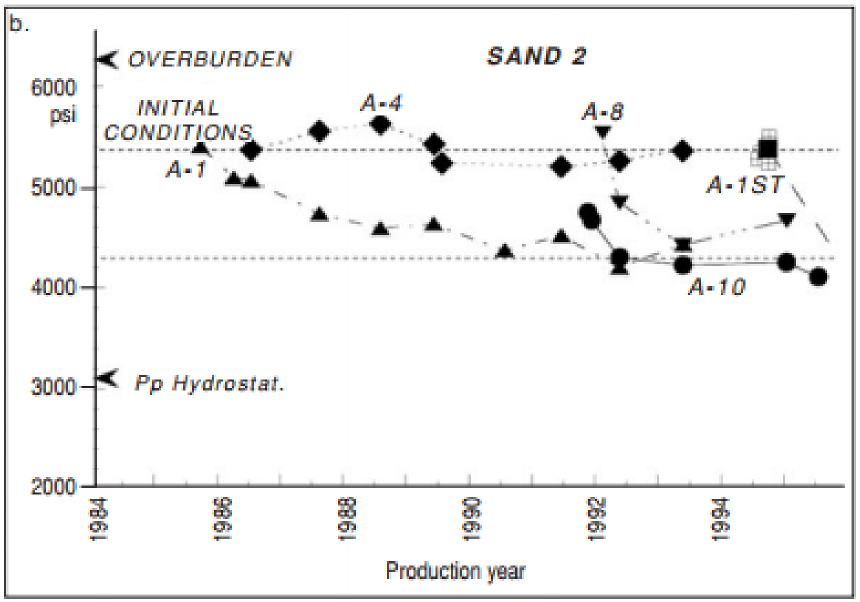

- P_p responds very differently
- Compartmentalized at a smaller scale than the mapped faults

Zoback MD, 2007, Reservoir Geomechanics, Cambridge University Press

Reservoir Compartmentalization
Pore pressure **variation** within compartments (2)

SEOUL NATIONAL UNIVERSITY

- Miocene sand in Southern Louisiana
  - The role of sealing fault

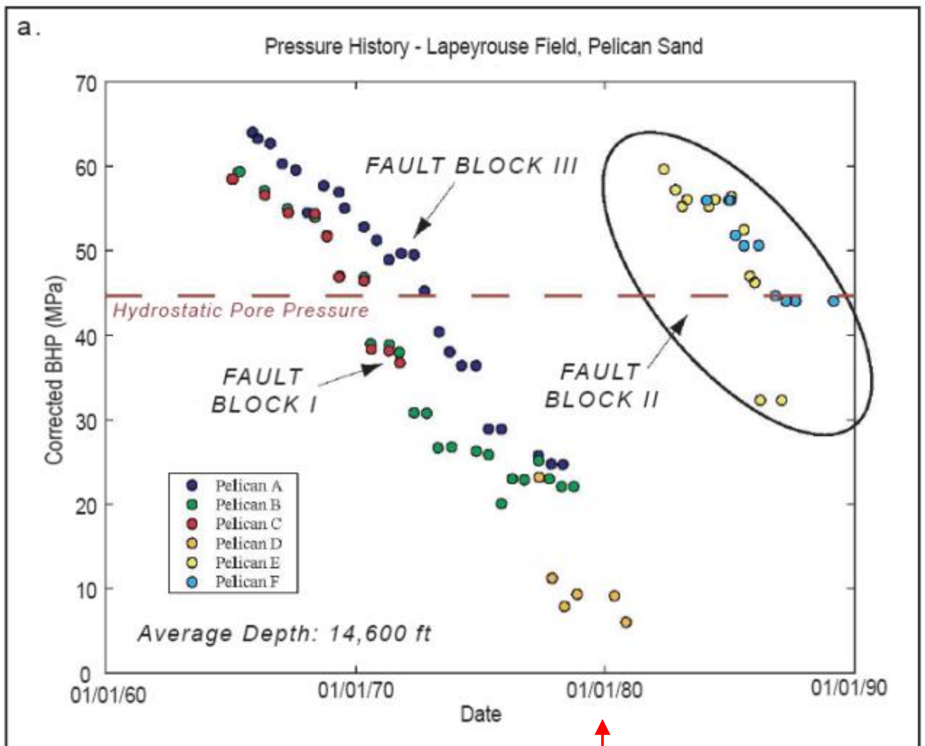

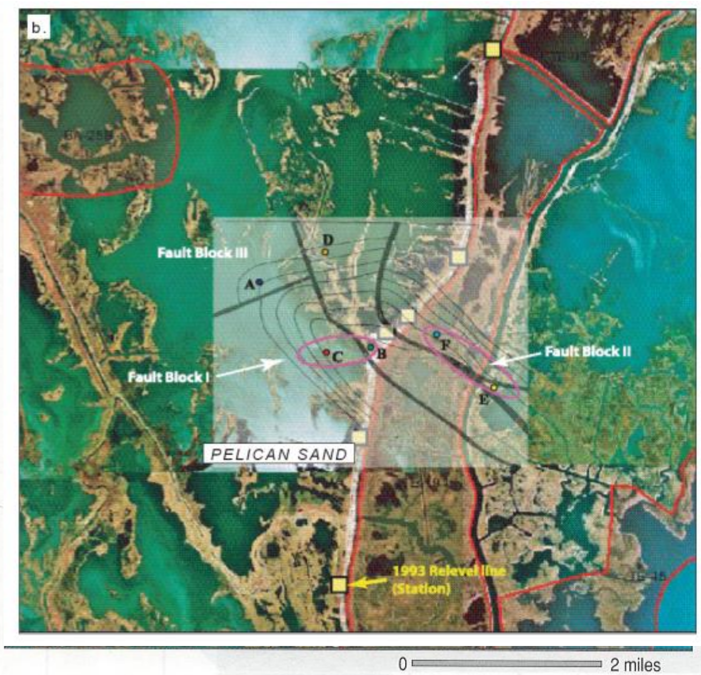

Figure 2.10. The Pelican sand of the Lapeyrouse field in southern Louisiana is highly compartmentalized. Note that in the early 1980s, while fault blocks I and III are highly depleted, fault block II is still at initial reservoir pressure (modified from Chan and Zoback 2006). Hence, the fault separating wells E and F from B and C is a sealing fault, separating compartments at pressures which differ by ~55 MPa whereas the fault between wells B and C is not a sealing fault.

Zoback MD, 2007, Reservoir Geomechanics, Cambridge University Press

Mechanisms of overpressure generation

SEOUL NATIONAL UNIVERSITY

- Underpressure is rare → will not discuss
- Mechanisms of overpressure
  - Disequilibrium compaction
  - Tectonic compression
  - Hydrocarbon column heights
  - Centroid effects
  - Aquathermal pressurization
  - Dehydration reaction
  - Hydrocarbon generation

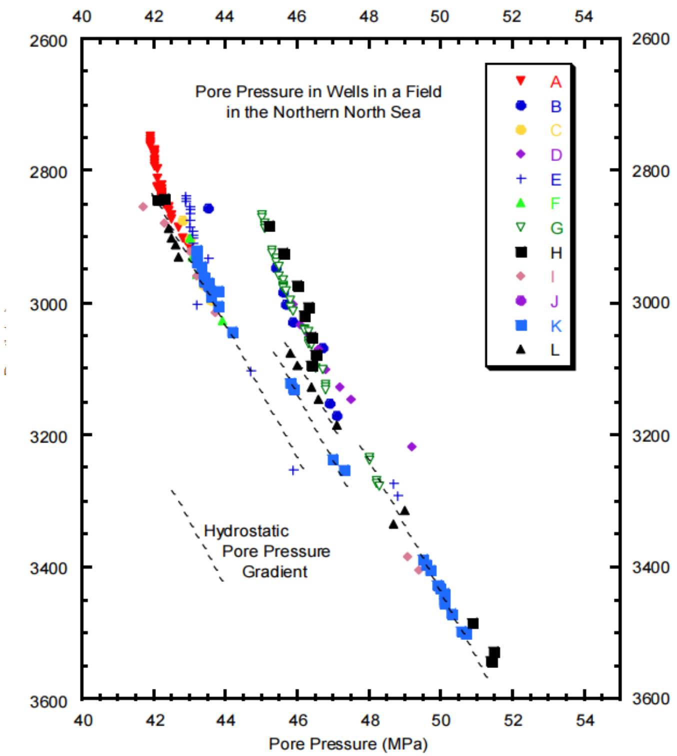

Figure 2.11. Pore pressure measurements from an oil and gas field in the northern North Sea. Note the distinct, low gradient, hydrocarbon *legs* associated with reservoirs encountered in a number of wells.

Zoback MD, 2007, Reservoir Geomechanics, Cambridge University Press

Mechanisms of overpressure generation
Disequilibrium compaction (undercompaction)

SEOUL NATIONAL UNIVERSITY

- Compaction under high/low permeability system
  - High permeability
    - Speed of compaction is comparable to permeability → no overpressure



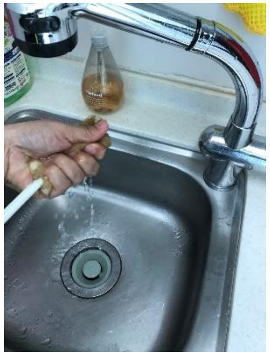

  - Low permeability
    - Speed of compaction is too fast compared to permeability → overpressure generation



Mechanisms of overpressure generation
Disequilibrium compaction (undercompaction)

SEOUL NATIONAL UNIVERSITY

- Characteristic time for linear diffusion

storativity

$$\frac{k}{\mu}\cdot\left(\frac{\partial^2 p}{\partial x^2}+\frac{\partial^2 p}{\partial y^2}+\frac{\partial^2 p}{\partial z^2}\right) = S\,\frac{\partial p}{\partial t}$$

$$\frac{\partial^2 p}{\partial x^2}+\frac{\partial^2 p}{\partial y^2}+\frac{\partial^2 p}{\partial z^2} = \frac{\mu S}{k}\cdot\frac{\partial p}{\partial t} = \frac{1}{c}\,\frac{\partial p}{\partial t}$$

$$S = \phi\beta_f + \beta_r \approx \phi\beta_f$$

$$\beta_f \approx 5\times10^{-4}/\mathrm{MPa} = 5\times10^{-10}/\mathrm{Pa}$$

$$\mu\ (\eta) \approx 10^{-3}\ \mathrm{Pa\cdot s} = 1\ \mathrm{cp}$$

Diffusion equation
Dimensional Analysis

SEOUL NATIONAL UNIVERSITY

- Dimensionless group dictate the nature of diffusion process or demonstrate the competition between two rate process

$x^+ = x/L$
$y^+ = y/L$
$z^+ = z/L$
$t^+ = t/t_e$
$h^+ = h/h_e$
$\nabla^+ = L\nabla$
$\nabla^{2+} = L^2\nabla^2$

+ indicates a dimensionless quantity
L : some characteristic length
t_e : some characteristic time
h_e : some characteristic head

L: length of the model (1D) or some length associated with fluid movement (2D)

$$\nabla^2 h = \frac{S_s}{K}\frac{\partial h}{\partial t} \longrightarrow \nabla^{2+} h^+ = \left(\frac{S_s L^2}{K t_e}\right)\frac{\partial h^+}{\partial t^+}$$

$$\nabla^2 p = \frac{\mu S}{k}\frac{\partial p}{\partial t}$$

$$\nabla^{2+} p^+ = \frac{\mu S}{k}\cdot\frac{L^2}{t_e}\cdot\frac{\partial p^+}{\partial t^+} = \tau\cdot\frac{1}{t_e}\frac{\partial p^+}{\partial t^+}$$

$$\tau = \frac{l^2}{\kappa} = \frac{(\phi\beta_\mathrm{f} + \beta_\mathrm{r})\eta l^2}{k} \qquad (2.2)$$

η

where l is a characteristic length-scale of the process, $\kappa \approx k/(\phi\beta_\mathrm{f} + \beta_\mathrm{r})$ is the hydraulic diffusivity, β_f and β_r are the fluid and rock compressibilities, respectively, ϕ is the rock porosity, k is the permeability in m^2 ($10^{-12}\ \mathrm{m}^2 = 1$ Darcy), and η is the fluid viscosity.

1 D (darcy) = $0.987\times10^{-12}\ \mathrm{m}^2 \sim 10^{-12}\ \mathrm{m}^2$

Mechanisms of overpressure generation
Disequilibrium compaction (undercompaction)

- Characteristic time for linear diffusion

$$\log \tau = 2\log l - \log k - 16 \tag{2.3}$$

(7))

$$\log \tau = 2\log l - \log k + \log(\overset{10^{-3}}{\mu} \cdot (\overset{0.2}{\phi}(\beta_f + \overset{5\times10^{-10}}{\beta_r})))$$

$$= 2\log l - \log k - 13$$

$l = 0.1\,km = 100\,m$

i) $k = 1\,mD = 10^{-15}\,m^2$.

$\log \tau = 2\times2 + 15 - 13 = 6$.

$\tau = 10^{6}$ sec. $=$ 0.03 years.

ii) $k = 10^{-20}\,m^2$.

$\tau = 10^{11}$ sec $=$ 3170 years.

- Sandstone (high k): short diffusion time
- Shale (low k): long diffusion time

Mechanisms of overpressure generation
Disequilibrium compaction (undercompaction)

SEOUL NATIONAL UNIVERSITY

- Permeability vs. hydraulic diffusivity

Diffusion Equation

Porous media fluid flow

$$\frac{\partial^2 p}{\partial x^2} + \frac{\partial^2 p}{\partial y^2} + \frac{\partial^2 p}{\partial z^2} = \underbrace{\frac{\mu S}{k}}_{\frac{1}{c}} \cdot \frac{\partial p}{\partial t}$$

c : hydraulic diffusivity

Heat conduction

$$\frac{\partial^2 T}{\partial x^2} + \frac{\partial^2 T}{\partial y^2} + \frac{\partial^2 T}{\partial z^2} = \underbrace{\frac{\rho C}{k}}_{\frac{1}{c}} \frac{\partial T}{\partial t}$$

c : thermal diffusivity

permeability : k $\qquad q = -\frac{k}{\mu} \cdot \frac{dp}{dx}$

hydraulic diffusivity : $\kappa = \frac{k}{\mu \cdot (\phi \beta_f + \beta_r)}$

Mechanisms of overpressure generation

SEOUL NATIONAL UNIVERSITY

- Tectonic compression
  - Occur in a similar manner as compaction
  - Locations under tectonic compression (high Pp in compression, low Pp in extension) - Coast ranges of California, Cooper basin in central Australia, North Sea
- Hydrocarbon column heights
- Centroid effects
- Aquathermal pressurization:
  - pore pressure expansion due to radioactive decay

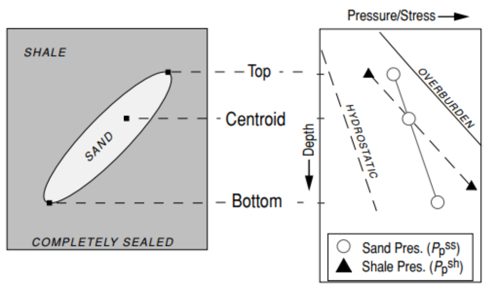

Figure 2.12. Illustration of the centroid effect where the tilting of a sand body encased in a low permeability shale results in a higher pore pressure at the top of the sand than in the shale body at the equivalent depth (from Finkbeiner, Zoback *et al.* 2001). *AAPG© 2001 reprinted by permission of the AAPG whose permission is required for futher use.*

- Dehydration reactions
  - Mineral diagenesis (expulsion of water from crystal lattice of montmorillonite…)
- Hydrocarbon generation
  - Thermal maturation of kerogen in hydrocarbon source rock

*kerogen: organic matter in sedimentary rock

Zoback MD, 2007, Reservoir Geomechanics, Cambridge University Press

Estimation of Pore pressure at depth
Direct measurement & Importance of estimation

SEOUL NATIONAL UNIVERSITY

- Direct measurement
  - Wireline logging
  - Through drill pipe
- Mud weights are also indicator of Pp
- Importance of estimating Pp
  - Estimation from seismic reflection data before drilling
  - Direct measurement of Pp at impermeable rock is difficult

Direct measurement of Pore pressure by wireline logging (Rider & Kennedy, 2011)

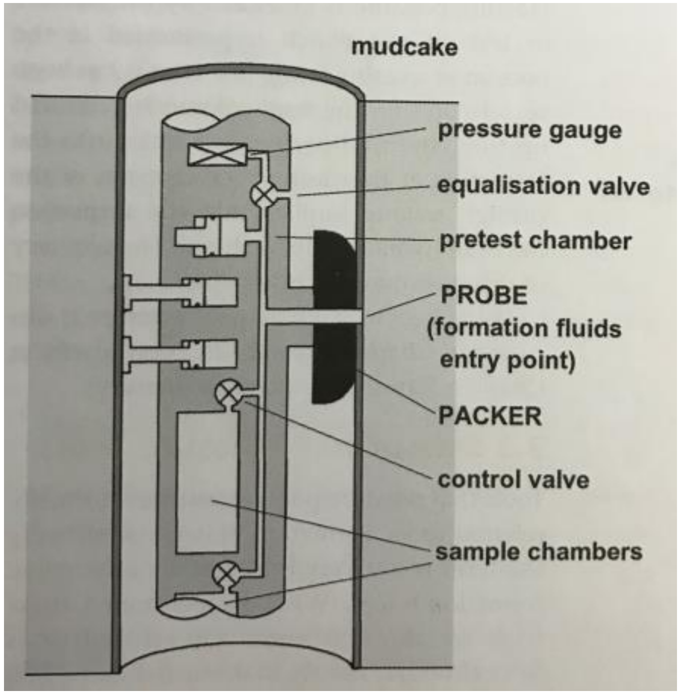

Rider M and Kennedy M, 2011, The geological interpretation of well logs, 3rd ed., Rider French

Estimation of Pore pressure at depth
Estimation from Porosity

SEOUL NATIONAL UNIVERSITY

- Underlying physics - Porosity decrease with the increase of (vertical) effective stress (Sv-Pp)
- Example of shale (Fig.2.13)
  - Overburden gradient: 23 MPa/km, Vertical effective stress gradient: 13 MPa/km
  - Porosity ←logging, sonic velocity, or resistivity
  - Example1) Φ=0.17 at 2 km depth
  - Example 2) Φ=0.26 at 2 km depth

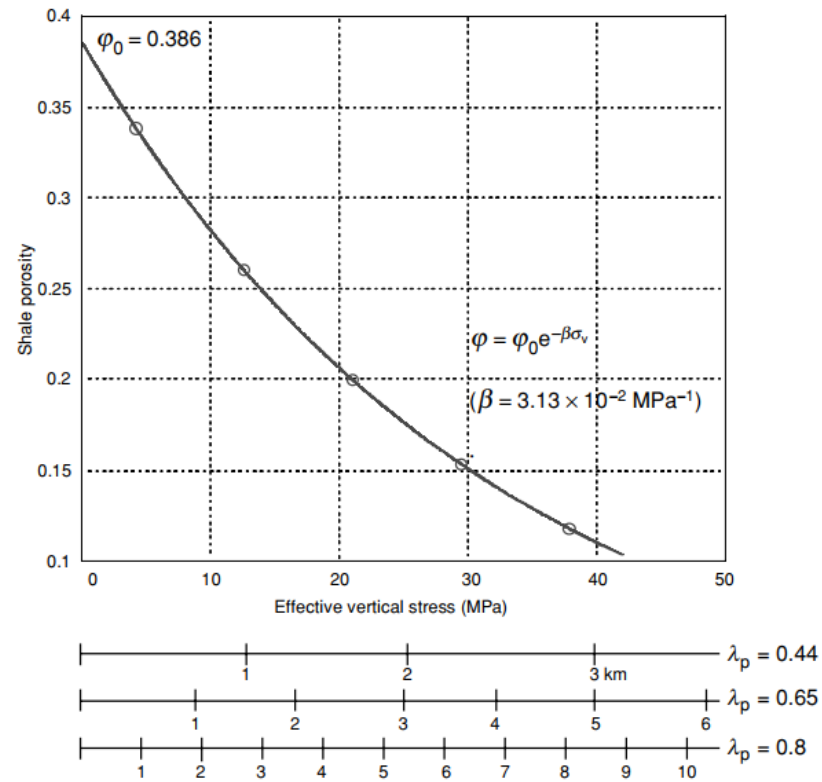

Figure 2.13. The decrease in porosity with effective stress in a SEI-330 shale sample subject to confined uniaxial compression test (Finkbeiner, Zoback *et al.* 2001). The effective stress refers to the difference between the applied uniaxial stress and pore pressure.

$$\phi = \phi_0 e^{-\beta\sigma_v} \tag{2.4}$$

where the porosity, ϕ, is related to an empirically determined initial porosity ϕ_0. σ_v is simply the effective stress

Zoback MD, 2007, Reservoir Geomechanics, Cambridge University Press

Estimation of Pore pressure at depth
Estimation from Porosity

SEOUL NATIONAL UNIVERSITY

- Abnormally high porosity at a given depth can be used to infer the presence of overpressure

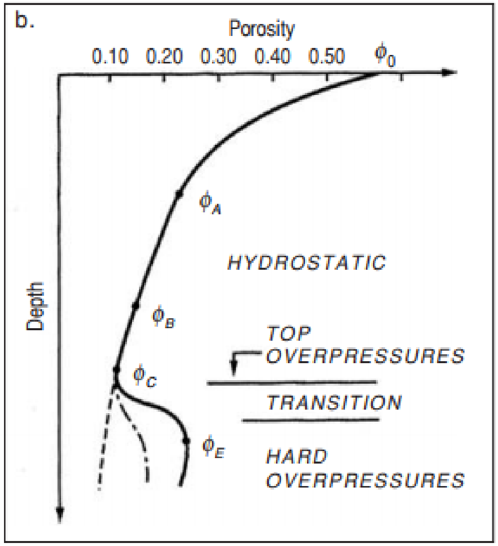

Figure 2.14. At depths A, B and C where pore pressure is hydrostatic (as shown in (a)), there is linearly increasing effective overburden stress with depth causing a monotonic porosity reduction (as shown in (b), after Burrus 1998). If overpressure develops below depth C, the vertical effective stress is less at a given depth than it would be if the pore pressure was hydrostatic. In fact, the vertical effective stress can reach extremely low values in cases of hard overpressure. Geophysical data that indicate abnormally low porosity at a given depth (with respect to that expected from the *normal* compaction trend) can be used to infer the presence of overpressure. *AAPG© 1998 reprinted by permission of the AAPG whose permission is required for futher use.*

Zoback MD, 2007, Reservoir Geomechanics, Cambridge University Press

Estimation of Pore pressure at depth
Estimation from Resistivity/sonic velocity

SEOUL NATIONAL UNIVERSITY

- Resistivity & sonic travel time Δt(P wave velocity V_p^{-1}) can be used to estimate Pp

$$P_p^{sh} = \left(S_v - P_p^{hydro}\right)\left(\frac{1-\phi_v}{1-\phi_n}\right)^x \tag{2.5}$$

where x is an empirical coefficient, ϕ_v is the porosity from shale travel time, ϕ_n is the expected porosity from the *normal* trend, and P_p^{hydro} is the equivalent hydrostatic pore pressure at that depth. Because resistivity measurements can also be used to infer porosity, Traugott has also proposed

$$P_p^{sh} = Z\left[\frac{S_v}{Z} - \left(\frac{S_v}{Z} - \frac{P_p^{hydro}}{Z}\right)\left(\frac{R_o}{R_n}\right)^{1.2}\right] \tag{2.6}$$

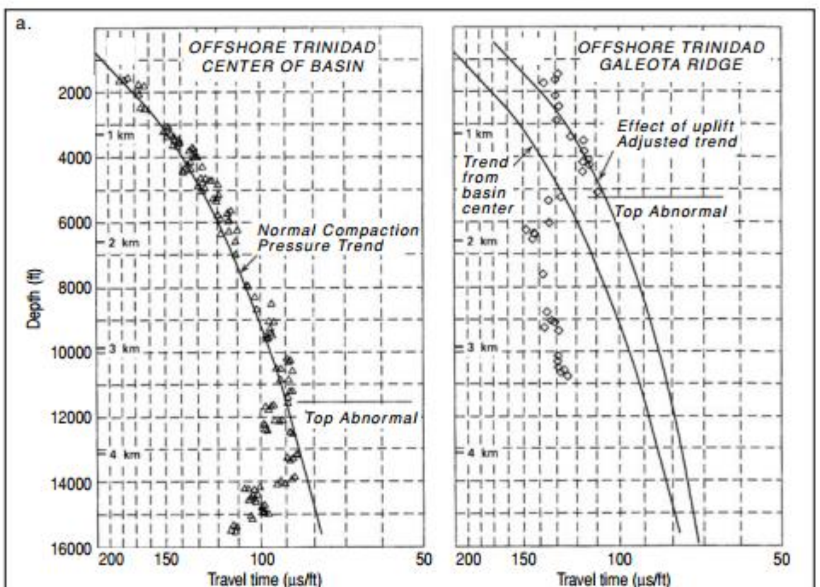

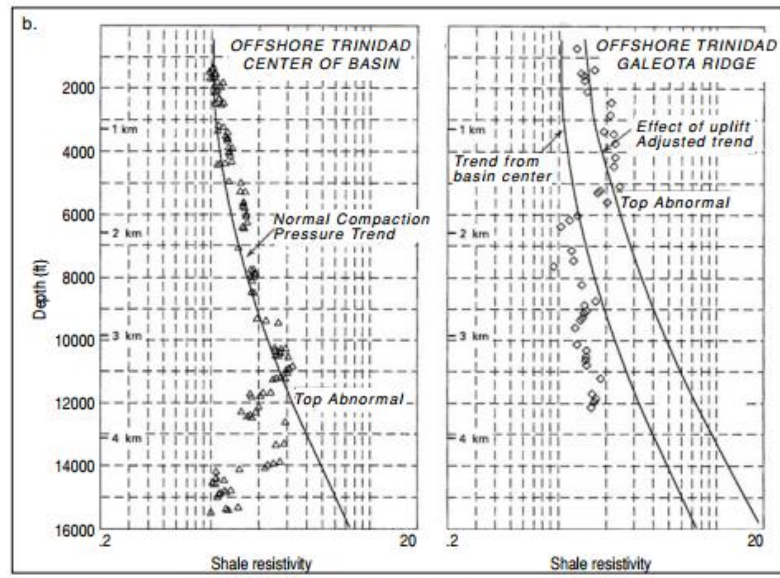

Figure 2.15. Data indicating compaction trends in Trinidad as inferred from (a) travel time data and (b) resistivity data (from Heppard, Cander *et al.* 1998). Assuming that the deviations from the normal compaction trends is evidence of overpressure (abnormally low effective stress), both sets of data indicate an onset of overpressure in the center of the basin at ~11,500 ft and 5,200 ft in the vicinity of the Galeota ridge. *AAPG© 1998 reprinted by permission of the AAPG whose permission is required for futher use.*

Zoback MD, 2007, Reservoir Geomechanics, Cambridge University Press

Estimation of Pore pressure at depth
Estimation from seismic reflection data

SEOUL NATIONAL UNIVERSITY

- Estimation of Pp from seismic reflection data prior to drilling

$$V_{\mathrm{i}} = 5000 + A\sigma_{\mathrm{v}}^{B} \tag{2.9}$$

(Bowers 1994) where V_{i} is the interval velocity (in ft/sec), A and B are empirical constants and $A = 19.8$ and $B = 0.62$ (Stump 1998). Because σ_{v} increases by about 0.93 psi/ft, this leads to

$$P_{\mathrm{p}} = 0.93z - \left(\frac{V_{\mathrm{i}} - 5000}{19.8}\right)^{\frac{1}{0.62}} \tag{2.10}$$

where the depth, z, is in feet.

Measured velocities

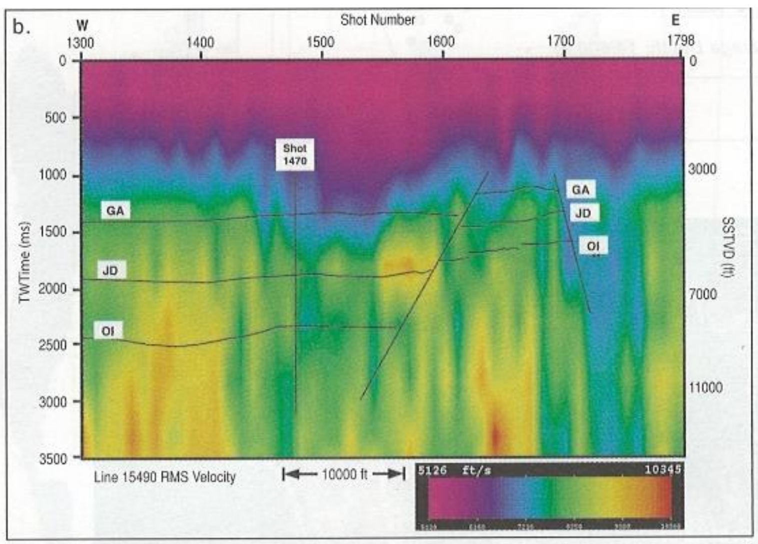

Inferred pore pressure

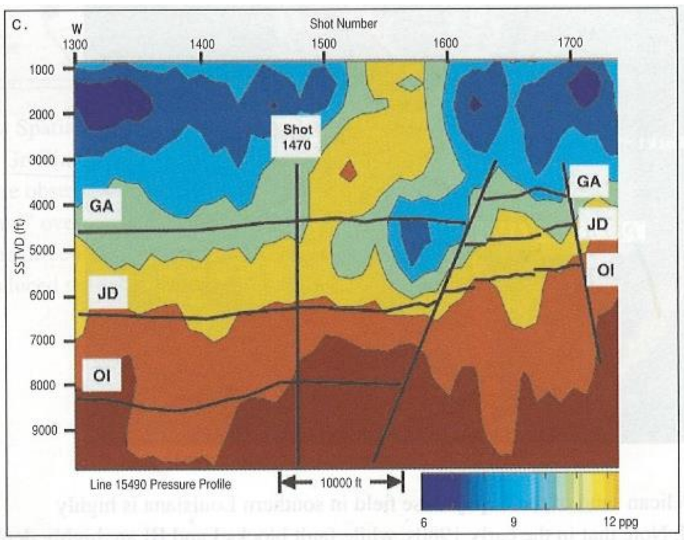

Figure 2.17. Pore pressure estimation from seismic reflection data along an E–W seismic line in the SEI-330 field (after Dugan and Flemings 1998). (a) Stacking, or RMS, velocities determined from normal moveout corrections. (b) Interval velocities determined from the RMS velocities. (c) Pore pressures inferred from interval velocity in the manner discussed in the text.

Zoback MD, 2007, Reservoir Geomechanics, Cambridge University Press

Estimation of Pore pressure at depth
Cautions

SEOUL NATIONAL UNIVERSITY

- Complicating factors
  - Estimation applicable to shale but not in sands and carbonates
  - Other factors may have affected (other than effective stress)
  - How to relate the lab data to field (scale, pressure, role of horizontal stress…)
  - Complex burial history and unloading

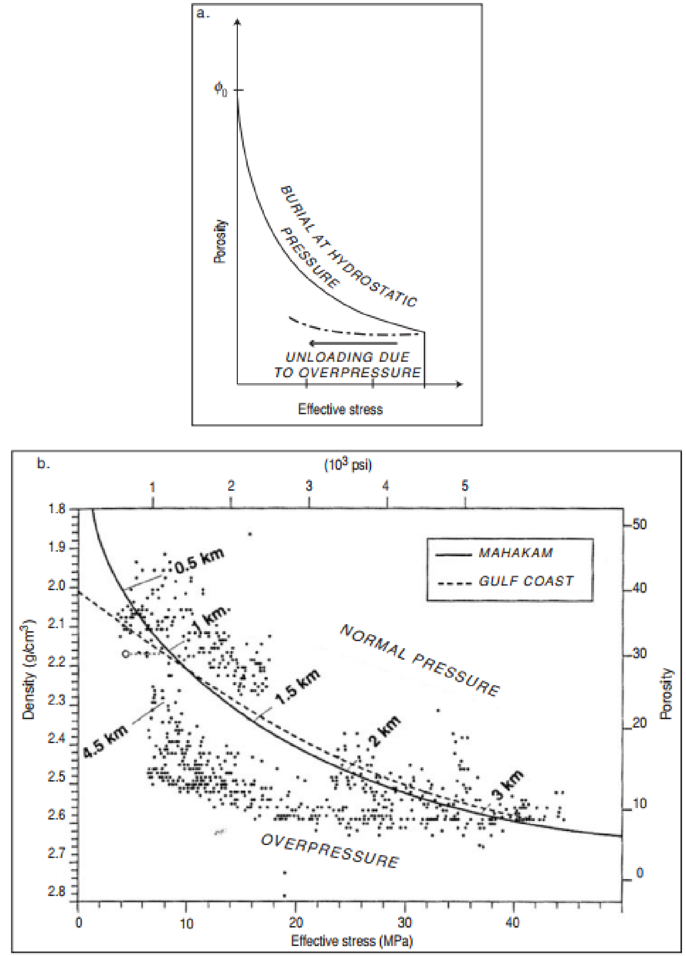

Figure 2.18. (a) Schematic illustration of the small porosity *recovery* that occurs upon unloading in weak sediments. Thus, if the current state of a reservoir represents a formation that has been unloaded, a nearly constant porosity is observed over a wide range of effective stresses (i.e. pore pressures). (b) Field data from the Mahakam Delta (Burrus 1998) which demonstrate that because overpressure at depths > 3 km developed after burial, the relation between porosity and effective stress during loading makes it difficult to infer pore pressure from porosity during unloading (see text). *AAPG© 1998 reprinted by permission of the AAPG whose permission is required for futher use.*

Zoback MD, 2007, Reservoir Geomechanics, Cambridge University Press